Journal of Environmental Radioactivity 222 (2020) 106347

Contents lists available at ScienceDirect

Journal of Environmental Radioactivity

journal homepage: http://www.elsevier.com/locate/jenvrad

Dynamics of radionuclide activity concentrations in weed leaves, crops and of air dose rate after the Fukushima Daiichi Nuclear Power Plant accident

Sergey Fesenko [a,*], Takuro Shinano [b], Yuichi Onda [c], Gerd Dercon [d]

[a] Russian Institute of Radiology and Agroecology, Obninsk, Kaluga region, 249020, Russian Federation
[b] Hokkaido University, Laboratory of Plant Nutrition, Kitaku, Sapporo, 060-8589, Japan
[c] Center for Research in Isotopes and Environmental Dynamics, University of Tsukuba, Tsukuba, 305-8572, Japan
[d] Joint FAO/IAEA Division of Nuclear Techniques in Food and Agriculture, International Atomic Energy Agency, IAEA, A-1400, Vienna, Austria

ARTICLE INFO

Keywords:
FDNPP accident
Radioiodine
Radiocaesium
Weed
Buckwheat
Rice
Soy bean

ABSTRACT

Data on reduction of radioactivity in plants are highly important for making decision on emergency response and remediation of contaminated areas. Dynamics of the ^{131}I and ^{137}Cs concentrations in the weed leaves sampled in the areas affected by the Fukushima Daiichi Nuclear Power Plant (FDNPP) accident in Japan was assessed for the period March–December 2011. The effective half-lives for ^{131}I and ^{137}Cs of 3.8–4.2 days and 7.1–13.3 days in the weed leaves were calculated for the first two months after the deposition. The approach for assessment of the aggregated transfer factors based on the ambient dose equivalent rate was suggested and validated. The geometric means of the soil to the weed leaves aggregated transfer factors were estimated for June–December 2011. Soil to crop ^{137}Cs- concentration ratios (buckwheat, brown rice and soybean) were estimated for 2011–2016. Soil to crop concentration ratios were found to decrease in the order of soybean > buckwheat > brown rice. The effective half-lives for ^{137}Cs in these crops were estimated to be between 1 and 2.5 years for the period 2011 2016, and longer than 5–7 years after 2016. It was found that these data comply with the Chernobyl related data obtained for similar conditions and complement of international documents on radionuclide transfer in agricultural environment such as the IAEA TRS 472.

1. Introduction

The accident at the Fukushima Daiichi Nuclear Power Plant (FDNPP) in Japan in 2011 gave rise to the widespread deposition of radioiodine (^{131}I) and radiocaesium (^{137}Cs and ^{134}Cs) throughout surrounding prefectures up to 500 km from the power plant. The Fukushima prefecture was most seriously affected and received approximately 80% of the total fallout deposited at the Japanese territory (Kato et al., 2019).

Assessment of radionuclide transfer in the environment always includes a consideration of the reduction of radionuclide activity concentrations in vegetation over the course of time after release of radionuclides (Takeda et al., 2013). After a nuclear accident, contamination of vegetation including agricultural crops, declines markedly resulting in large changes in the radionuclide activity concentrations in foodstuffs and, sequentially, in internal doses to the public. Large changes are also observed for the air dose rates due to decay of short-lived radionuclides and radionuclide redistribution among environmental compartments, because of weathering of radionuclides originally intercepted by plants and radionuclide transfer to the top soil and their lixiviation to lower soil (Fesenko et al., 1996; IAEA, 2010). Distribution of radionuclides in the environment could also be affected by the various farming activities (Alexakhin et al., 2007).

Time-dependent behaviour of radionuclides in the environment is often quantified by application of the ecological half-life, which is a lumped parameter equal to the time, over which radionuclide concentrations, in some component of a trophic chain, are decreased by a factor of two, without account for radioactive decay (IAEA, 2010).

Although field-based data on dynamics of radionuclide concentrations obtained after single depositions are limited, there are several sources of information on the dynamics of radionuclides in the environment, including: the global fallout, the Kyshtym, Chernobyl and Fukushima Daiichi accidents. These data are invaluable for environmental model development.

The global fallout, with maximum depositions observed in 1962–1964, represented a variable source of the radionuclides for the environment (Uchida and Tagami, 2007). Research carried out

* Corresponding author.
E-mail address: corwin_17f@mail.ru (S. Fesenko).

https://doi.org/10.1016/j.jenvrad.2020.106347
Received 14 February 2020; Received in revised form 19 June 2020; Accepted 28 June 2020
Available online 2 August 2020
0265-931X/© 2020 Elsevier Ltd. All rights reserved.

following the accidents at the "Mayak" nuclear reprocessing plant (Kyshtym accident) happened in autumn and did not generate a lot of information on behaviour of radionuclides in the environment during the early phase after the depositions (Alexakhin et al., 1996). Some valuable information on short-term dynamics of radionuclides in plants was attained after the Chernobyl accident and these data were used in most of the dynamic environmental models developed in the past 30 years (Alexakhin et al., 2007).

A unique situation for the evaluation of environmental dynamics of radioiodine and radiocaesium for both short and long-term periods appeared after the Fukushima Daiichi NPP accident: the well-known release resulted in high activity concentrations of radionuclides in a wide range of the affected environments with different soils, land use, farming practices. The Fukushima environmental monitoring programme with a special focus on air dose, radionuclides concentrations in the soil and in vegetation was started on 18 March 2011 by the Emergency Operation Center (EOC) operated by the Environmental Radioactivity Monitoring Center of Fukushima (MEXT, 2012a; MEXT, 2012b; Onda et al., 2015, 2020).

The radionuclide transfer from the soil to the plants is often quantified by the soil to plant concentration ratios.[1] However, an application of this parameter to describe the uptake of radionuclides by vegetation has been subject to some criticism (Simon and Ibrahim, 1987; Sheppard and Evenden, 1988). Initially designed for application in agricultural ecosystems, the soil to plant concentration ratios were considered to be unsuitable for usage in natural pastures where the soil is unploughed, and the radionuclides studied are not uniformly distributed with soil depth (Sanzharova et al., 1994). However, the transfer factor (or soil to plant concentration ratio concept) remains an important component of many dose assessment models, and for that reason was applied as part of this study.

It can be expected that the data on radionuclide concentrations in the plants can reflect radionuclide transfer to the plants consumed by animals and humans whilst ambient dose rates can be used as a proxy for the external exposure of the population. Indeed, the weed leaves are often considered as analogues of leaf vegetables that can directly contribute to the other crops to the internal dose to the public (Onda et al., 2020) and on the other hand can be considered as an analogue for the natural grasses that can be consumed by grazing animals. Thus, the dynamics of the plant contamination together with data on the external dose rates can be directly used for making decisions in emergency response in agriculture (Khomutinin et al, 2020a; 2020b).

The Fukushima environmental monitoring programme with special focus on the air dose, the radionuclides concentrations in the soil and vegetation started on 18 March 2011 by the Emergency Operation Center (EOC) operated by the Environmental Radioactivity Monitoring Center of Fukushima (MEXT, 2012a; MEXT, 2012b; Onda et al., 2015, 2020). The soil and vegetation samples were taken in a variety of different locations in the areas affected by the Fukushima Dai-ichi NPP (Onda et al., 2015, 2020). Further, in 2011, the MAFF organized a sampling campaign for measurement of radiocaesium in rice on the paddy fields selected based on expert judgements. Such sampling was significantly expanded from 2012 onwards (Shinano et al., 2020).

Some input data used in this research was also presented by Renaud et al. (2012) and Onda et al. (2020). Renaud et al. (2012) provided a discussion of the site selection and the data for study site, whereas Onda et al. (2020) provides details of the sites and the sampling campaign. However, no estimations of radionuclides half-lives in the weed leaves were made based on these data. Thus, data evaluation and analysis presented in this paper are very different from those presented in the above publications.

The purpose of the paper was to quantify a reduction of the radionuclide concentrations in the weed leaves that were considered as a representative for the natural vegetation, in the crops (buckwheat, rice and soybean) and dynamics of the air dose rates and to provide important lessons learned for improving response to nuclear emergencies affecting food and agriculture. The paper chronologically considers time dependent issues related to emergency response in agriculture, including dynamics of 131I, 134Cs, 137Cs in the weed leaves, radiocaesium transfer to weed leaves upon completion of deposition and reduction in 137Cs concentration ratios to crops afterwards.

2. Materials and methods

2.1. Soil and plant sampling

2.1.1. Weed leaves

Following the FDNPP accident, a comprehensive monitoring of radionuclide activity concentrations in the weed leaves was initiated by the Emergency Operation Centre (EOC) operated by the Environmental Radioactivity Monitoring Centre of Fukushima. Soil and vegetation samples were taken in a variety of different locations in the areas affected by the Fukushima Dai-ichi NPP (Onda et al., 2015, 2020). Fifteen sampling sites were defined where samples of the soils and the weeds leaves, were collected in March–December 2011 (MEXT, 2012a; MEXT, 2012b). The soil and vegetation sampling was constantly supplemented by the air dose rate measurement at 1 m height above ground. Overall, the sampling sites covered the environmental conditions specific for this part of Japan. Each row in the sampling database includes information on the sampling site, the sampling date, the result of the air dose measurements, the concentrations of ^{131}I, ^{134}Cs and ^{137}Cs and also the data on the same other radionuclides, if detectable. The dates of sampling supplemented with the information on dates of the major deposition events can be easily converted to the time from the deposition providing basis for time dependent assessments.

The weed species at the sites were presented by the Rosette family plants, namely, *Rumex obtusifolius*, *Dandelion, Plantain, Goldenrod, Papaver dubium*. These plants are considered as a potential analogue to leafy vegetables i.e., can be used as a proxy for internal dose assessments (Onda et al., 2020).

Sampling of the weed leaves, the soil and the air dose measurements were carried out on a daily basis for the first few weeks and, depending on the location, the time between two sampling events was lengthened to 3–5 days later. The samples of the weed was measured in a fresh mass basis without sample preparation (Onda et al., 2020).

A detailed description of the sampling procedure is described elsewhere (Onda et al., 2015, 2020) whilst this section provides a summary to facilitate the paper reading. Sampling sites were selected outside of the 10-km zone of the FDNPP, additional to the predetermined sampling points within the 10-km zone. Due to a lack of resources, a simplified version of the official sampling protocol was implemented for sampling of the weed leaves (Onda et al., 2020). The sampling campaign included daily sampling of plants (around 400 g fresh mass) and soils (around 800 g fresh mass). The samples were taken with longer intervals when the patterns of the dynamics of radionuclide activity concentrations in plants were established. Although the official sampling campaign was started on 7th April 2011, some samples were collected as early as 17-18th March 2011 (Onda et al., 2020).

Sampling sites with respect to the FDNPP are shown in Fig. 1, whereas timing and location of the main deposition events are shown in Fig. 2. Information presented in Figs. 1–2, makes it possible to estimate time of the major deposition events specific for the weed leaves sampling sites. These and other data available for the sampling sites (Onda et al., 2015, 2020) are summarised in Table 1.

The sites can be split into three groups based on times between the major deposition events and start of the sampling campaign (see Fig. 2). The dates of the start of sampling at the sites varied from 18th March (sites 2-1 - 2–6) to 4th April 2011. The first group of the sites (sampling

[1] For purposes of this paper, the terms soil to plant concentration ratio, and transfer factors from soil to plants are used interchangeably.

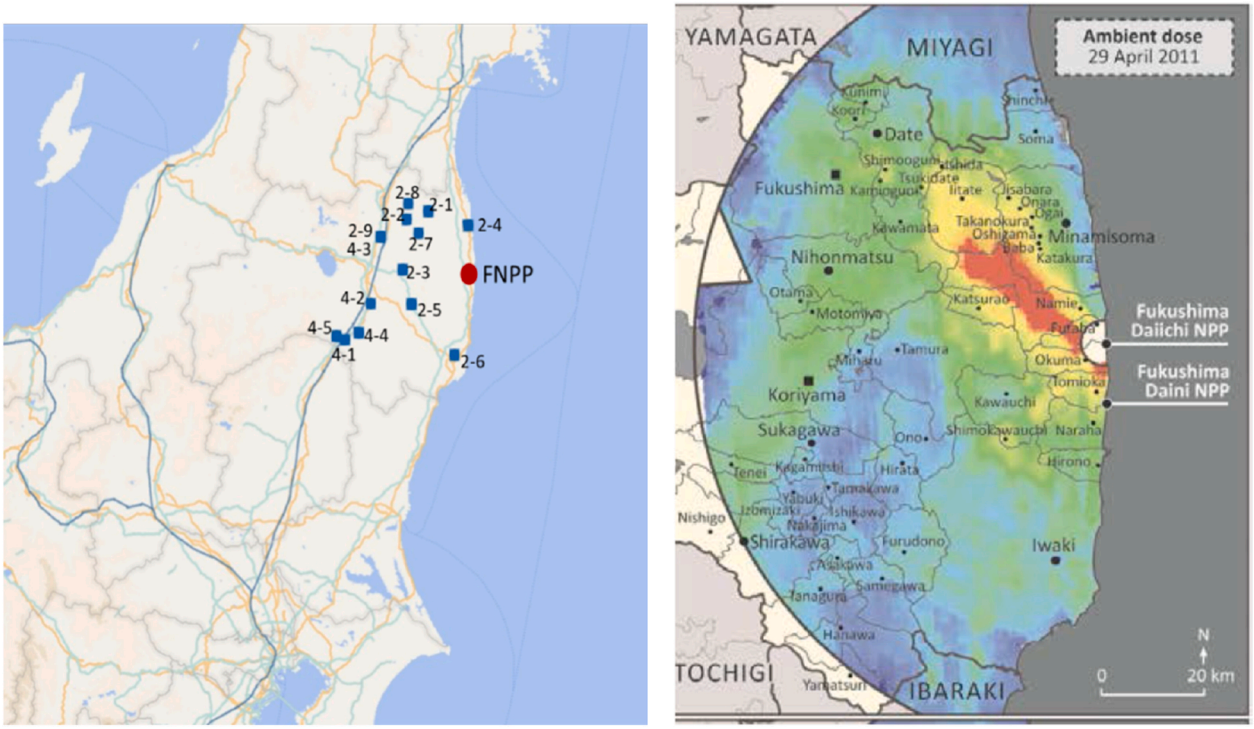

Fig. 1. Locations of the sampling sites in respect to the areas affected by the FdNPP.

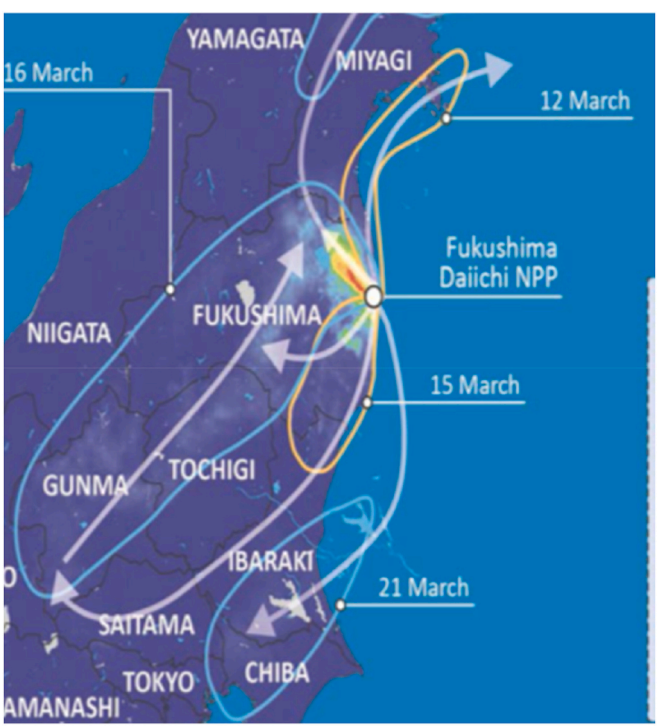

Fig. 2. Timing and location of the main deposition events (MEXT, 2011; Nagai et al., 2012).

sites 2-1 - 2–6) includes sites where observations (i.e. sampling and ambient dose rate measurements) started a few days after the deposition events. The second group (sites 2–7 - 4.1) are the sites where the time interval between the major deposition event and start of the sampling was approximately two physical half-lives of ^{131}I, and the third group of the sites included the sites where the time interval between the major deposition event and beginning of the observation was three physical half-lives of ^{131}I. The dynamics of radionuclide in plants reflected the difference between time of the start of the monitoring programme and the deposition event and such differences were considered for assessing half-lives of radionuclides in the weed leaves.

2.1.2. Crops

Estimating the C_r values for the crops was based on the sampling provided by the Ministry of Agriculture, Forestry and Fisheries (MAFF). In March 2011, most of the crops were not being sown yet and the plants were not directly contaminated by the Fukushima depositions. Only some representative fields were selected for sampling and if the concentration of rice in the bags exceeded the provisional regulation value, total investigation of such fields was carried out. Therefore, the data of combined radionuclide activity concentrations in the crops at the time of harvest and corresponding data on the air dose rate was rather limited and included information on radiocaesium (separately for ^{134}Cs and ^{137}Cs) in the rice and the air dose rate for individual fields (Fukushima prefecture, 2011).

Furthermore, starting from 2012, the sampling campaign for measuring radiocaesium in the crops (rice, buckwheat and soy bean), the soil and the air dose rates at the fields used in agriculture was significantly expanded. The database included information on the field location number, the name of the crop, the date of harvest, the ^{134}Cs and ^{137}Cs activity concentrations in the crop and the soil, the exchangeable potassium concentrations on the dates of planting and harvest as well as results of the air dose rate measurements. The crops were sampled at the time of harvest according to the existing sampling guide recommended for such a purpose by the MAFF (Shinano et al., 2020). Thus, the soil to plant concentration ratios for the crops produced in the Fukushima prefecture and associated ambient dose rates were assessed based on the data presented elsewhere (Shinano et al., 2020).

2.2. Ambient dose equivalent rate measurements

The air (ambient) dose rate measured at the height of 1 m above the topsoil is an important parameter that can be used for radiological

Table 1
Characteristics of the sampling sites near the Fukushima Daiichi NPP in 2011.

Site ID	Group of sites	Location	Distance from the FDNPP	Date of depositions	Start of sampling	Number of sampling points
2–1	1	Iitate village	42 km North/West	2011/03/16	2011/03/22	75
2–2	1	Kawamata town	45 km North/West	2011/3/16	2011/3/25	77
2–3	1	Tamura city Funehiki	41 km West	2011/3/16	2011/3/18	75
2–4	1	Minamisoma city Haramachi	24 km North	2011/3/15	2011/3/25	74
2–5	1	Tamura city Ono	39 km West/South/West	2011/3/15	2011/3/18	75
2–6	1	Iwaki city Taira	43 km South/South/West	2011/3/15	2011/3/18	75
2–7	2	Kawamata town	34 km West/North/West	2011/3/16	2011/3/25	65
2–8	2	Date city Tsukidate	50 km North/West	2011/3/16	2011/3/25	68
2–9	2	Nihonmatsu city Kanairo	57 km West/North/West	2011/3/16	2011/3/25	68
4–1	2	Shirakawa city	80 km North	2011/3/16	2011/3/25	18
4–2	3	Sukagawa city Hachiman	60 km West/South/Wes	2011/3/16	2011/4/7	18
4–3	3	Otama village	60 km West/North/West	2011/3/16	2011/4/7	53
4–4	3	Zumizaki village	72 km West/South/West	2011/3/16	2011/4/7	18
4–5	3	Nishigo village	84 km West/South/West	2011/3/16	2011/4/8	17

assessments. For the purposes of this paper, the terms of "air dose rate", used in the MEXT documents (MEXT, 2012a; 2012b) and "ambient dose equivalent rate" are used interchangeably. The sampling of the weed leaves and the soils was supplemented by the ambient dose measurements. The air dose rates at the sites were measured at a height of 1 m above the ground at the time of sampling using CsI(TI) scintillation detectors (Onda et al., 2015). The same approach was used for air dose measurements at the fields occupied by crops, including paddy fields in 2011 and fields with buckwheat, rice and soybean in 2012–2016.

2.3. Data analysis and quality control

Soil to plants aggregated transfer factor values for the radiocaesium concentrations in the weed leaves were calculated as the radionuclide activity concentrations of ^{137}Cs (Bq/kg in the weed leaves, FW) per unit area activity density (A_a, in kBq/m^2). The soil to crops concentration ratios considered in the study, such as rice, buckwheat, soybeans were reported as a ratio of the radiocaesium activity concentration in the crop (Bq/kg, DM) to the activity concentration in the soil (Bq/kg, DM).

Normally, the data for each sampling point included data for both radiocaesium isotopes, radioiodine (for the first two months after the deposition), the air dose rates and some other fields' attributes. During the initial data check, the rows that had uncomplete sets of attributes, such as missed data for one of radiocaesium isotopes or the air dose rates were eliminated from the further analysis. Therefore, the number of the data for every sampling point used for further assessments were normally less than that given for same sampling points published in the MEXT, 2012a and MEXT 2012b.

To evaluate the calculated soil to plant C_r values, statistical methods appropriate for small sample sizes were used (Geras kin et al., 1994). The tiered procedure for initial data evaluation was applied:

The ratio of ^{134}Cs–^{137}Cs in samples of soil and plants was served as a tool for data quality checks as there is no disequilibrium in environmental behaviour of these isotopes.

- For each combination of year/soil/crop, detection criteria were used to identify any outlier values that were eliminated.
- Following the elimination of outliers, characteristics of the probability distribution were identified. For the estimation of the distribution density parameters, the Mieses criterion, modified for small data sets, was used (Geras kin et al., 1994).
- Normal statistical methods were used for large data sets. As soil to plant concentration ratios are often found to follow a log-normal distribution (Sheppard and Evenden, 1988, 1990); this was checked for each dataset first.

Identification of outliers was an important step in assessing environmental data. Based on this statistical procedure, the outlier values were either withdrawn from the original dataset or these values were undergone for analysis in depth to identify the factors contributing to the data deviation from the expected trends.

The Microsoft Excel, Statistica 9.0 and Grapher 9.6 standard software packages were used for the statistical analysis, the calculations of effective half-lives and the graphical presentations of the data reported in the paper.

3. Results and discussion

3.1. Preliminary data analysis

The isotopic ratios ^{131}I/^{137}Cs and ^{134}Cs/^{137}Cs calculated based on the MEXT data are given in Table 2. Despite the uncertainties with the assessments of the releases from the FDNPP, the estimates of ^{131}I and ^{137}Cs releases are quite consistent with the literature data (UNSCEAR, 2013; IAEA. 2015; Chaisan et al., 2013).

The geometric mean ^{134}Cs/^{137}Cs isotopic ratio recalculated for the time of the first release was found to be about 1.0; this value perfectly complies with that given in the IAEA Fukushima report of 2015 (IAEA, 2015). Thus, the data demonstrate that both caesium isotopes were present in the environmental samples in very similar quantities. Based on that, the data where only one caesium isotope was measured in the sample were withdrawn from further analysis. Overall, the MEXT website provides 776 rows for the March–May sampling campaign (MEXT, 2012a). In 135 cases (17%), the concentrations of both caesium isotopes were not detected. In 41 samples (5.2%) ^{134}Cs was not detected, although ^{137}Cs was measured, whilst in 6 cases (0.77%), ^{134}Cs was detectable but Cs^{137} was not.

Table 2
Isotopic ratios of ^{131}I and ^{134}Cs–^{137}Cs recalculated to 15 March of 2011 based on the weed leaves sampling after the FDNPP accident.

Sites	^{131}I/^{137}Cs			^{134}Cs/^{137}Cs		
	G. Mean	G. St. Dev.	Correl. Coeff.	G. Mean	G. St. Dev	Correl. Coeff.
2–1	15.1	3.0	0.62	1.0	1.0	0.99
2–2	5.0	1.5	0.78	1.0	1.1	0.99
2–3	6.6	1.9	0.92	1.0	1.2	0.99
2–4	27.7	2.1	0.67	1.0	1.1	0.99
2–5	16.4	2.1	0.94	1.0	1.2	0.99
2–6	67.8	1.6	0.87	1.0	1.1	0.99
2–7	8.76	1.8	0.95	1.0	1.1	0.99
2–8	4.7	1.4	0.96	1.0	1.1	0.99
2–9	7.1	1.6	0.91	1.0	1.1	0.99
4–1	10.1	1.1	0.90	1.0	1.0	0.99
4–2	11.0	1.8	0.9	1.0	1.0	0.99
4–3	11.0	1.5	0.89	1.0	1.0	0.99
4–4	16.5	1.0	0.69	1.0	1.1	0.99
All sites	11.8	2.0		1.0	1.0	

The variations of the isotopic ratios $^{131}I/^{137}Cs$ were higher than those observed for caesium isotopes. These can be explained by the different times of release, the different deposition velocities, and the different contributions of wet and dry depositions at the sampling sites. Therefore, the higher deviations of the ratios $^{131}I/^{137}Cs$ was not considered as a reason for data withdrawal but rather as a signal for deeper data analysis.

The $^{131}I/^{137}Cs$ ratios recalculated to 15 March 2011 looks a bit more uncertain compared to that for the ratio of caesium isotopes. Short half-life and, hence, low ^{131}I concentrations in environmental samples after the first few weeks after depositions could contribute to the variability of the data observed.

High correlations ($R^2 \sim 0.99$) were observed for two caesium isotopes, whereas correlation between ^{131}I and ^{137}Cs was somewhat lower. It can be explained by the different forms of these radionuclides in the atmosphere, with possible overlapping of the depositions released at different times from the different FDNPP units.

The geometric mean of 11.2 with the geometric standard deviation around that mean of 2.0 for the isotopic ratios of $^{131}I/^{137}Cs$ were calculated based on the data of Table 2. The isotopic ratio of $^{134}Cs/^{137}Cs$ for individual sampling sites was very close to 1.0 and was fully consistent with all other release data, confirming overall good performance of the sampling campaign.

High correlation coefficients between concentrations of caesium isotopes, and for most sites also between the concentrations measured for ^{137}Cs and ^{131}I, allow a designation of ^{137}Cs as a reference radionuclide and replace, if required, concentrations of other dose-forming radionuclides with ^{137}Cs, making corrections for differences in radioactive decay coefficients.

Natural background external dose rate can also contribute to the dose rates especially at the sites with a low deposition after the FDNPP accident. Indeed, the contribution of natural outdoor radioactivity ranged from 1 to 30%, reaching 30% at sites 2–3, 2–4, 2–5, 2–6 and 4-2. High contributions of natural radioactivity (10–15%) can also be noted for sites 2–10 and 4-4.

3.2. Half-lives of ^{131}I, ^{134}Cs and ^{137}Cs in the weed

The data on dynamics of radionuclides in the weed leaves are presented in Figs. 3–4, whilst corresponding effective and ecological half-lives are given in Table 3.

A general observation relevant to all radionuclides and the sites involved, is the tendency of an increase of activity concentrations in the weed leaves following 40 days after the beginning of sampling, when activity concentrations were much lower compared to those detected during the first sampling days. Therefore, the half-lives given in Table 3

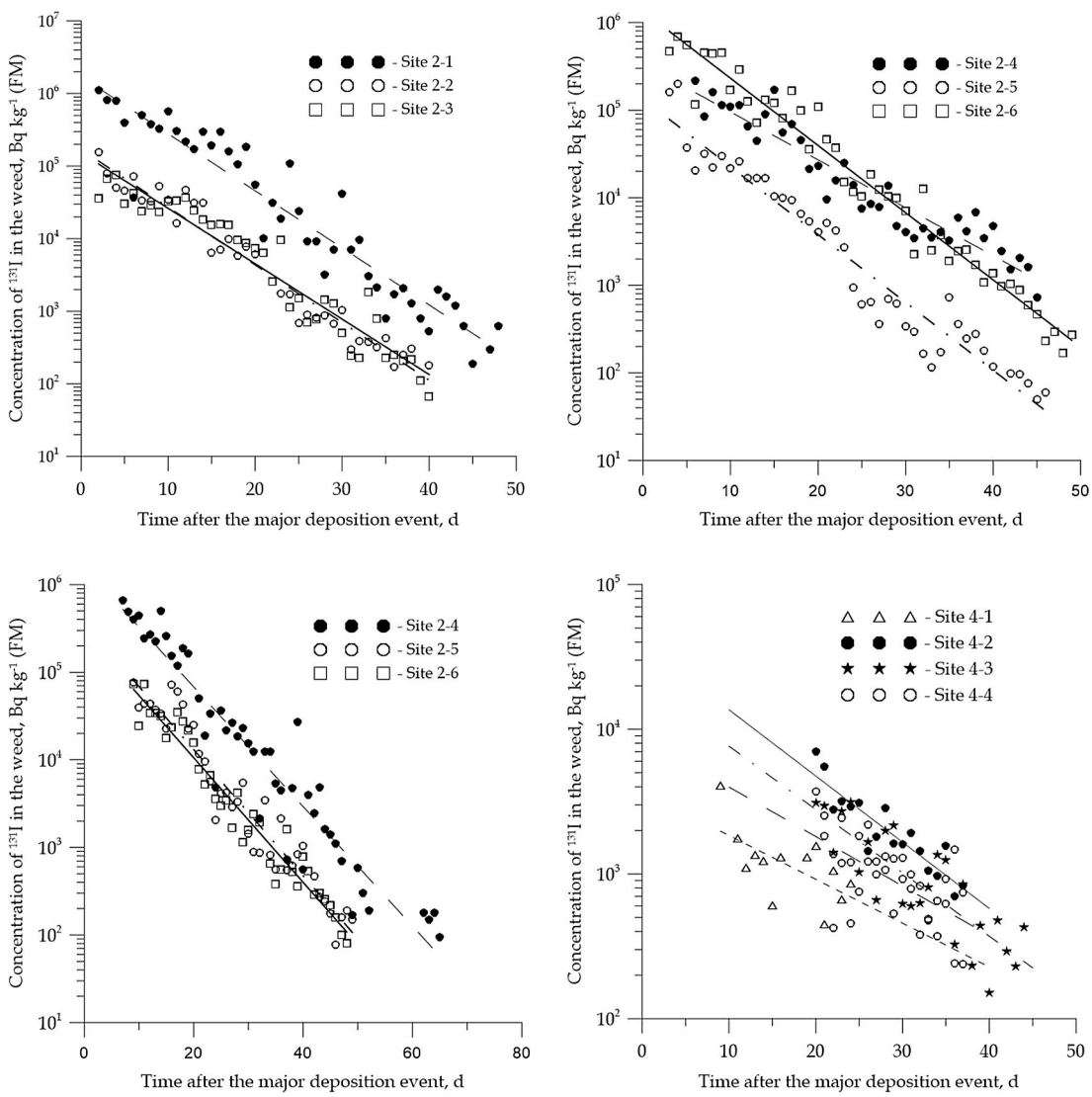

Fig. 3. Dynamics of the ^{131}I activity concentrations in the weed leaves after the FDNPP accident.

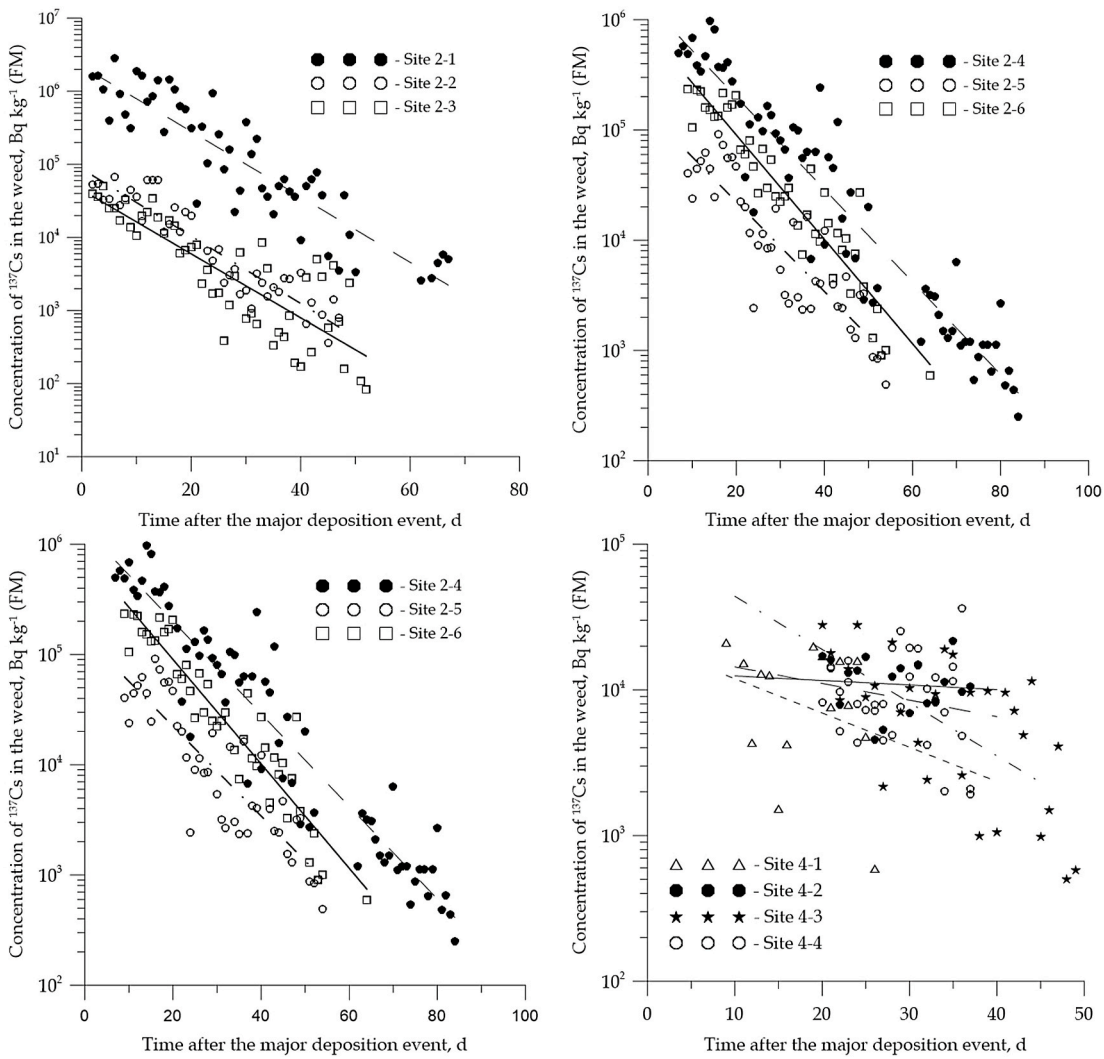

Fig. 4. Dynamics of the ^{137}Cs activity concentrations in the weed leaves after the FDNPP accident.

Table 3
Half-lives of ^{131}I and ^{137}Cs isotopes in the weed leaves.

Sites	^{131}I			^{137}Cs	
	$T_{1/2}$., d[a]	$T^{e}_{1/2}$, d[b]	R^2	$T_{1/2}$, d	R^2
2–1	3.8 (3.8)[c]	7.2 (7.2)	0.89 (0.9)	8.56	0.80
2–2	3.8 (4.0)	7.2 (7.9)	0.96 (0.87)	12.2	0.62
2–3	3.9 (4.0)	7.7 (8.0)	0.92 (0.92)	9.00	0.73
2–4	5.5 (7.9)	17.5 (451)	0.91 (0.92)	13.3	0.77
2–5	3.8 (3.9)	7.3 (7.6)	0.94 (0.94)	8.3	0.76
2–6	3.9 (4.4)	7.6 (9.7)	0.96 (0.95)	13.08	0.83
2–7	4.2 (4.4)	8.7 (9.7)	0.92 (0.90)	7.14	0.90
Mean for Group 1	3.9	7.6		9.7	
2–8	4.2 (4.3)	8.8 (9.2)	0.93 (0.91)	10.2	0.80
2–9	4.2 (4.6)	8.8 (10.7)	0.93 (0.91)	7.7	0.85
Mean for Group 2	4.2	8.8			
4–1	9.9	42.2	0.4	13	0.084
4–2	6.9	29.4	0.83	99	0.083
4–3	6.9	29.4	0.7	12	0.4
4–4	8.8	37.5	0.38	27	0.038
Mean for Group 3	8.1	34.7		38	

[a] Effective half-life.
[b] Ecological half-life.
[c] Half lives calculated based on all available information are given in brackets.

were calculated based on data for the first 40 days after the depositions, whereas half-lives calculated based on all available data (typically 60 days after the depositions) are given in brackets. A possible explanation could be a transfer of radionuclides intercepted by trees to the topsoil (Kato et al., 2012, 2017), and the resuspension of the deposited radionuclides from the area with higher contamination levels around the sampling point (Hirose, 2013).

The most striking point is the exceptionally long half-life of ^{137}Cs in the weed leaves sampled at the site of 2–4. The ecological half-life calculated based on the data taken from the whole sampling time i.e. from 18 March to 31 May 2011 is more than 400 d. The ecological half-life calculated based on data for the first 40 days after the depositions gives a shorter value of 17.5 d, which is also much longer than those observed for the other sites. Considering the values for site 2–4 as the outliers, effective and ecological half-lives calculated for the rest sites of the first two groups varied in a narrow range. Thus, the effective half-lives for ^{131}I, ranged 3.8–4.2 d for the first group (where observations started a few days after the major deposition event) and 4.2 d for the second group, where observation started later. The mean value for the first group of sites was estimated to be 3.9 d with the standard deviation around that mean of 0.15. Both values for sites of the second group are 4.2 d and, hence, the mean value was also 4.2 d.

The effective half-life values calculated for sites 4-1-4-4 are nearly two-fold higher than those estimated for sites of the first and the second groups. The interpretation of these results should consider the fact that

the observations at sites of the third group started 20 days after the deposition. It is known that the two-component loss model is the best option in fitting dynamics of the ^{131}I concentrations in plants. Therefore, these values can be interpreted as the data providing an estimate of the second half-life of the two-component loss model. Although values of the coefficient of determination (R^2) tend to be above 0.9 for the first group's sites, these values ranged 0.38–0.7 for the remaining sites, demonstrating higher deviation of the results of the observations around fitting curves.

The effective half-lives for radiocaesium were generally longer than those calculated for ^{131}I and ranged 7.4–13.8 d. Although observations made for ^{131}I are also valid for ^{137}Cs, the coefficient determination values calculated based on the exponential fit for the sites 4-1 - 4-4 are statistically insignificant. High variations in the data and short observation periods do not allow a justification of the relevant statistical models to describe these data.

The weathering half-life values estimated for both ^{131}I and ^{137}Cs are consistent with similar data measured after the Chernobyl accident (IAEA, 2006). Measurements of radioiodine in plants after the Chernobyl accident allowed the estimation of the mean ecological half-life as 8.8 d with the range around that mean of 2.8–15 d. As for ^{137}Cs, the mean ecological half-life in plants was 17.0 d with the range of 9.0–34 d (IAEA, 2006). Wide ranges for the Chernobyl weathering half-life values were mainly due to the higher diversity of the environmental conditions in the areas where the Chernobyl related data were obtained.

3.3. Dynamics of air dose rate and soil to weed leaves 2011 and its applications

The reduction of the air dose rate provides valuable information for assessing consequences of the radioactive contamination. In the case of the FDNPP accident, this parameter played a major role for making decisions on setting of the contaminated areas with the appropriate status, evacuation of the population, decontamination of the settlements and remediation of the environment.

The reduction of the air dose rate (E_{air}, μSv h^{-1}), is a multi-factor process and can be described by a multi-exponential function. The reasons are different decay constants of iodine and caesium isotopes and redistribution of radionuclides in the environments, resulting in a change of the geometry of the radiation exposure. Such considerations are brought into the well-known equation for estimating ambient dose equivalent rate widely used for both Chernobyl (Golikov et al., 1999; Golikov et al., 2002; IAEA, 2006) and Fukushima affected areas (Takahashi, 2014; UNSCEAR, 2013):

$$E_{air} = r(t) * A_{137} * \ DCF(t) + E_{rb}, \quad \left(\frac{\mu Sv}{h}\right) \tag{1}$$

$$DCF(t) = \sum_i \left(\frac{A_i}{A_{137}}\right) * K_i^{dep} * \exp(-\lambda_i * t), \quad (\mu Sv\ h^{-1})/\left(kBq/m^2\right), \tag{2a}$$

where *r(t)* (dimensionless) is a ratio of the air dose rate above undisturbed open ground to that of the reference geometry. The above ratio is the function that takes into account the deviation of the actual geometry of the radiation source from the reference one. In particular, this function accounts for the penetration of radionuclides in soil or weathering of radionuclides from the plant surface to the topsoil. *DCF*(t) ((μSv h^{-1})/(kBq/m^2)) is the dose conversion function that provides conversion from contamination density of 1 kBq m^{-2} to ambient dose equivalent rate for the plain radiation source. A_i (kBq/m^2) is the deposition density of radionuclide *i*, and λ_i (d^{-1}) is the decay constant of radionuclide *i*. K_i^{dep} ((μSv h^{-1})/(kBq/m^2)) is the dose-rate conversion coefficient for a reference depth distribution in soil of radionuclide *i*, i.e. it is the ratio of the air dose rate at a height of 1 m above the ground to the deposition density on soil (μSv/h)/(kBq/m^2). These values are 1.3×10^{-3}, 5.59×10^{-3} and 2.05×10^{-3} (μSv/h)/(kBq/m^2) for ^{131}I, ^{134}Cs and ^{137}Cs, respectively (IAEA, 2001, based on Eckerman and Ryman, 1993). For the virgin or undisturbed soil, the reference geometry is a plane radiation source and appropriate information can be found elsewhere (Eckerman and Ryman, 1993; Bellamy et al., 2019).

^{137}Cs was chosen as the reference radionuclide for the Fukushima affected areas, as recommended by the UNSCEAR (2013), because it was the most long-lived and radiologically significant radionuclide. Function *r(t)* is often called by the attenuation factor and is normally considered as the sum of two exponents (Golikov et al., 1999; Golikov et al., 2002, IAEA, 2006, UNSCEAR, 2013; Takahashi, 2014):

$$r(t) = p * \exp(-\lambda_1 * t) + (1-p) * \exp(-\lambda_2 * t), \tag{2b}$$

For the long-term assessment of the variations in ambient dose equivalent with the time because of penetration of radionuclide in the virgin (undisturbed) soil, the parameters p_1 and p_2 amount to 0.34 and 0.66, whereas λ_1 and λ_2 are 1.27×10^{-3} and 3.8×10^{-5} d^{-1}, respectively (IAEA, 2006; UNSCEAR, 2013).

It is worth mentioning that the above estimates of the parameters of Eq. (2) are made based on observations over a long time. Therefore, they may be a bit different from those mentioned earlier based on short-term data (during the first year after the deposition). Indeed, the attenuation of the ambient dose equivalent at the height of 1 m above the ground is affected by weathering and the growth of new biomass during the first few months after the accident, whilst afterwards, the attenuation is governed by the penetration of radionuclides in the deeper soil layers. Thus, for the short term after the deposition these parameters could be re-evaluated taking into account real variations in air dose rate with the time. The ratios of ^{131}I and ^{134}Cs concentration at the time of the accident to those of ^{137}Cs concentration in the weed leaves are presented in Table 2 and can be used for such purpose.

The average level of the terrestrial radiation in Japan measured before the Fukushima accident turned out to be about 0.056 μSv h^{-1} (Abe et al., 1980). However, a somewhat higher value of 0.078 μSv h^{-1} reported by Shinano et al. (2020) as specific for the Fukushima affected area was taken as the E_{rb} estimate.

Thus, the unknown parameters in Eq. (1) are A_{137}, i.e, the ^{137}Cs density depositions at the sites and parameters of the attenuation function that were estimated fitting Eq. (1) to the measured data of ambient dose equivalent rates given at the NRA web-site (MEXT, 2012a, 2012b) (Table 4). These data, along with the fitted curves are given in Fig. 5, whilst the parameters of Eq. (2), estimated based on these data, are given in Table 4.

It is clear that the data obtained for the first year after deposition given in Table 4 describes the short-term decrease of the ambient equivalent dose rate. The data of Table 4 show that for one component loss model (Sites 2-1, 2-2, 2–3 and 2–5) the half-lives varied in a narrow range 1.2–1.7 years, whereas the two component loss model with the first half life ranged 0.05–0.17 years and the second half life of 2.4 years was more appropriate for the rest of the sampling sites. Most likely, for such sites the reduction of radiocaesium concentrations in the weed leaves reflects fast processes affecting the ambient equivalent dose rate

Table 4
Parameters of the models describing dynamics of air dose rate in 2011 at the sampling sites (see Eqs. (1) and (2)).

Site	A_{137} (kBq/m^2)	p	T_1, years	T_2, years	R^2
2–1	952	1	1.7		0.89
2–2	167	1	1.4		0.81
2–3	31	1	1.3		0.77
2–4	52	0.2	0.05	2.4	0.76
2–5	26	1	1.4		0.83
2–6	32	0.3	0.3	2.4	0.64
2–7	459	0.45	0.06	2.4	0.78
2–8	212	0.6	0.04	2.4	0.79
2–9	257	0.55	0.19	2.4	0.78
4–3	97	0.35	0.17	2.4	0.43

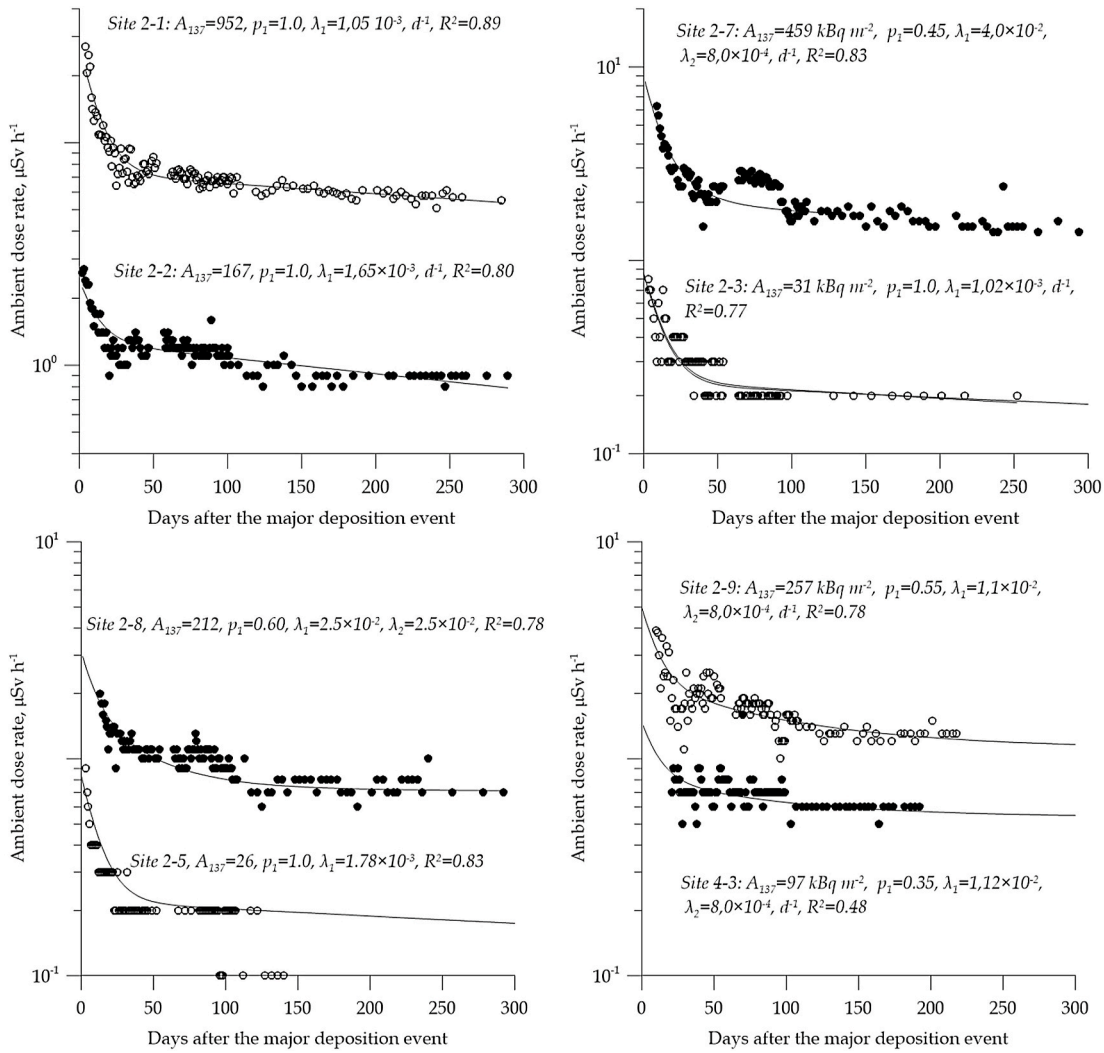

Fig. 5. Dynamics of the ambient dose equivalent rates at the height of 1 m above the ground measured at the sampling sites.

such as radionuclide weathering, growth new biomass attenuating the source and leaching of radiocaesium from the root mat and it's transfer to the top soil layer. It can also be seen from Fig. 5 that the data derived for low contaminated sites, namely, 2–3, 2–4, 2–5 and 2–6 exhibited contributions of the natural background that became significant after 40–60 days because of the decay of ^{131}I, which was a major contributor to the air dose rate during the first weeks after the depositions.

The most striking point is that the first half-lives of the attenuation function for most sites are very close to those assessed for the Chernobyl affected areas. This coincidence likely reflects the general patterns of the variations in the radiation source geometry after the deposition, whereas for other sites slightly more complex radionuclide redistribution in the first year was observed.

Yoshimura et al. (2020) recently reported data on the reduction of the ambient equivalent dose rates during the initial period after the accident measured at 103 points located outside a 20-km radius from the FDNPP since 15 March 2011. The research was a part of the monitoring program carried out by the MEXT and Nuclear Regulation Authority (NRA, 2011). The mean decrease rate due to the radionuclide migration of 0.17 year^{-1} was calculated as the difference between the decrease rates corresponding to radiocaesium decay and the observed data. The value of 0.17 year^{-1} corresponds to the half-life of 4.1 year.

This value suggests that the migration rate of radionuclide in the soil was smaller (or slower) in Fukushima than that observed in the Chernobyl affected lands. The half-life of 4.1 year presented by Yoshimura et al. (2020) is also longer compared to those observed for the sampling sites in our study.

There are two possible reasons for a long half-life presented in the study of Yoshimura et al. (2020) as follows. First, the data for the first 60 days were excluded from the Yoshimura et al. (2020) assessments. Secondly, the only data for the sites with the ambient dose equivalent rate lower than 0.1 μSv h^{-1} were eliminated from the mean reduction rated assessment. It is worth mentioning that the contribution of the radiation background could also affect dynamics of the air dose rates at the sites where the air dose was in the range of 0.1–0.5 μSv h^{-1}, where contribution of the natural background could also affect the measured air dose rates. These two assumptions made by Yoshimura et al. (2020) could contribute to longer estimates of the half-lives associated with the migration rate in the soil.

For estimating geometric mean of the deposition density at each site, the ratios of the ambient dose rates to the attenuation factors multiplied by dose conversion factors were calculated for each air dose rate data point available from the MEXT database (2012a, 2012b). (See Eq. (3)).

$$A_{137}\left(t\right) = \frac{E_{air}(t)}{(r(t)*DCF(t)} \tag{3}$$

Moving to a discreet approach adapted to the individual data points of the NARA (MEXT, 2012a; MEXT, 2012b) data base, Eq. (3) can be converted to the form:

$$A^{j}_{137}(t^{k}) = \frac{E^{j}_{air}(t^{k})}{r^{j}(t^{k}) * DCF^{j}(t^{k})}, \quad (4)$$

where index j corresponds to the sampling site and t^k is the time between the major deposition event and the date for which the ratio was calculated.

Based on these ratios the geometric means and geometric standard deviations of the ^{137}Cs contamination density values were calculated for each sampling site. Geometric means of the ^{137}Cs deposition densities, along with the data that combine the soil sampling at the sites and airborne survey (Onda et al., 2020), are given in Table 5.

The geometric mean values of A^{j}_{137} estimated based on ambient equivalent dose rate measurements, can potentially be more representative than individual soil sampling data because gamma-quants are gathered by the detector from rather large areas around the sampling point. Thus, time-dependent data of ambient dose equivalent rate can be used for retroactive calculations of the mean contamination densities of ^{137}Cs and, with the aid of the data of Table 2, these data also allows estimating contamination densities of ^{131}I and ^{134}Cs (Table 5).

A comparison of the estimates of ^{137}Cs deposition densities assessed based on different methods are shown in Fig. 6. The estimates based on geometric means of the air dose data are a little bit higher than geometric means based on the airborne survey, whereas the estimates based on arithmetic means are around 15% lower. Overall, this fact demonstrates high convergence of the estimates obtained by these methods and confirm a possibility to use air dose data for estimating deposition densities.

The striking point relevant to all sites is a perfect agreement of the ^{137}Cs contamination density values presented in Onda et al. (2020) and that of ambient dose equivalent rate measurements at the sites (Fig. 6). Another general point is that the correlation between geometric mean values based on air dose rate measurement and data from Onda et al. (2020) of 0.999 is higher than the correlation for arithmetic mean values of 0.952 based on air dose rate measurement. This serves additional evidence in preferences of using geometric mean versus arithmetic mean for estimating environmental parameters.

Based on the contamination density, the sampling sites can be split into two groups. The highly contaminated sites (2-1, 2-2, 2–8, 2–9 and 4-3), with the contamination density from 100 to 1000 kBq m^2 and the low contaminated sites where contamination density of ^{137}Cs ranged 10–100 kBq m^2. Such differences can substantially affect not only absolute values of the air dose rate but also the dynamics of the dose rates because of the different contribution of the natural radiation background. The presented data also demonstrates a possibility of realistic assessment of the contamination density at the sites of ^{131}I providing additional benefit for radiological assessments.

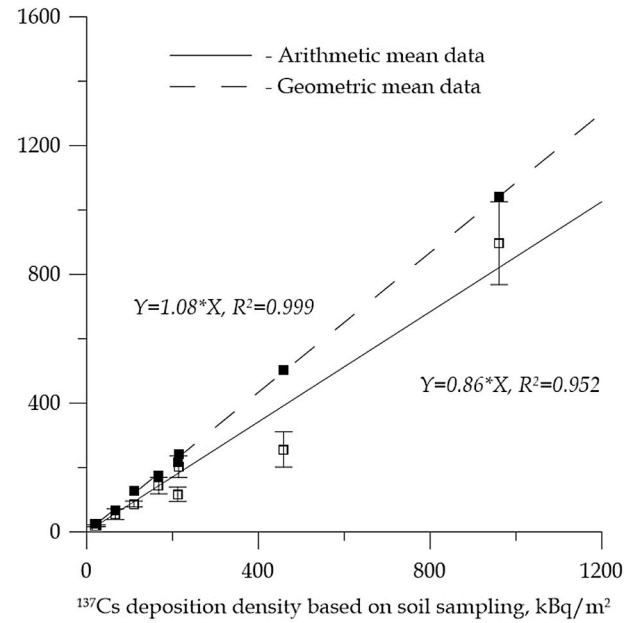

Fig. 6. Comparison of the estimates of ^{137}Cs contamination densities at the sampling sites presented in Onda et al. (2020) and ambient dose equivalent rate measurements.

3.4. Aggregated transfer factors from soil to weed from June–December 2011

Information on radionuclide concentrations in the animal products, such as milk, is of paramount importance for assessment of consequences of any radiological emergency. The farming practice in Japan normally includes keeping livestock indoors for a whole year. Conversely, some small farms producing milk mainly for local consumption can use pastures for grazing animals and this can lead to high internal doses to the public. In many countries animals are mainly grazing during summer when other feed is unavailable. That was the case in the summer of 1986, shortly after the Chernobyl accident, and can be observed in many countries with extensive agricultural systems. Therefore, assessment of contamination of pasture grass a few months after the deposition may be highly important and requires robust estimates of T_{ag} values from soil to vegetation.

The ^{137}Cs T_{ag} values for fresh grass were calculated individually for each date point where data for ambient dose equivalent rate and the concentration of ^{137}Cs in the weed leaves were available:

Table 5
Radionuclides deposition densities at the monitoring sites.

Site ID	Data from Onda et al. (2020)		Estimates based on ambient dose equivalent rate data				
	GM[a] of ^{137}Cs deposition, kBq m^{-2}	N[b]	^{137}Cs deposition, kBq m^{-2}		N[c]	^{131}I deposition, kBq m^{-2}	^{134}Cs deposition, kBq m^{-2}
			GM	GSD$_1$			
2–1	961	98	1042	1,2	137	1.5×10^4	1042
2–2	168	98	174	1,2	127	8.7×10^b	174
2–3	20	99	24	1,3	85	1.5×10^b	24
2–4	67	104	66	1,9	94	1.8×10^c	66
2–5	24	99	23	1,2	59	3.8×10^b	23
2–6	28	95	25	1,2	108	4.1×10^b	25
2–7	459	91	502	1,5	127	3.4×10^4	502
2–8	212	92	217	1,2	128	1.9×10^c	217
2–9	214	91	241	1,2	114	1.1×10^c	241
4–3	110		128	1,1	103	1.4×10^c	128

[a] GM is the geometric mean and GSD is the geometric standard deviation.
[b] Number of soil samples.
[c] Number of air dose rate measurements.

$$T^{j}_{ag}\left(t^{k}\right) = \frac{Q^{j}_{137}\left(t^{k}\right)}{A^{j}_{137}\left(t^{k}\right)} \quad (5)$$

Based on this approach, basic statistics of T^{j}_{ag} values specific for each sampling site were calculated, including geometric and arithmetic means, standard deviations and geometric standard deviations (Table 6).

The distributions of the T_{ag} values both for the whole dataset and for individual sites can be satisfactory fitted by the lognormal distribution (Fig. 7). This makes it a requirement to use geometric means for assessment of the T_{ag} values for comparisons with other data sets (Fig. 7).

Overall, the transfer factors do not show a statistically significant reduction for June–December 2011, although declining trends were observed for several sites (Fig. 8). A possible reason of this reduction is leaching of radiocaesium from the root mat. A rough estimate based on the exponential fit gave a half-life value of radiocaesium in the root mat of around 450 days. This value is a somewhat lower similar mean value observed in meadows in the near zone of the Chernobyl NPP of 533 days.

The individual T_{ag} values ranged 0.2–21.0 with mean value of 3.5 ± 1.7 (Bq/kg, FW)/(kBq/m^2) across all the sites. The geometric mean for the whole dataset was 2.3 (Bq/kg, FW)/(kBq/m^2). It is worth noting that the T_{ag} values are normally provided in the literature for the dry weigh. Therefore, the T_{ag} data estimated here (Table 6) were recalculated based on the value of 0.2 for dry matter content in pasture given in TECDOC 1616 (IAEA, 2009). The obtained values of 11.5 and 17.7 (Bq/(kBq/m^2), DM) are very close to the T_{ag} values of 15–25 (Bq/(kBq/m^2), DM) observed for the first year after the deposition in areas affected by the Chernobyl accident (Sanzharova et al., 1994). Although the property of the soils in the Chernobyl near zone and in the Fukushima affected areas are quite different, it can be speculated that the properties of the root mat are close, determining similar transfer rates from the root mat to the vegetation, and these data can be used for assessments in case of other potential accidents.

3.5. Soil to crops ^{137}Cs concentration ratios in 2012–2016

Evaluation of the half-lives of radionuclide in crops requires accounting for effect of variations with time of the soil parameters such as exchangeable potassium, pH, texture etc. (Yamamura et al., 2018). Implementation of remediation may also substantially contribute to the reduction of the C_r values (Fesenko et al., 2001). Some of the remedial options applied in the Fukushima affected area were focused on the changing of the soil properties (application of elevated dose of potassium fertilizers) and some of them included deep ploughing or topsoil removal that provide a mechanical reduction of radionuclide concentrations in the soil. In particular, a threshold value of 25 mg K_2O/100 g soil DM was applied for selecting fields for application of additional K^+ to reduce radiocaesium *CR* values for rice (MAFF, 2013). Lack of accounting for the effects of these factors can lead to additional uncertainty in the estimates of concentration ratios. Thus, the data used for soil to plant concentration ratio assessments reflect on-going environmental conditions, including soil properties mentioned earlier and the history of remedial actions implementation. Some examples of the C_r values to brown rice, buckwheat and soybean observed in 2012, 2014 and 2016 in respect to K_2O and ^{137}Cs concentrations in the soil are shown in Fig. 9.

The data demonstrate rather homogeneous C_r values excepting low contaminated fields with low concentrations of exchangeable K^+ in the soil. It is highly likely that potassium was not applied at such fields, and the C_r values were not reduced, as it was done on the highly contaminated fields where potassium was applied at the rates suppressing radiocaesium transfer to crops. Thus, these data serve as an evidence of effectiveness of remediation applied in the affected areas after the Fukushima Daiichi accident and can be best explained by potassium application to the paddy fields (Shinano et al., 2020). It should be emphasised that activity concentrations of radiocaesium in the crops planted in the fields with the C_r values are relatively low and do not pose any risk in terms of food safety.

The data for buckwheat and soybean demonstrate similar trends. The lowest ^{137}Cs C_r values to buckwheat and soybean were observed in areas with the high exchangeable potassium content in the soil and in the areas where potassium fertilisers were applied. This example also demonstrates the effect of application of potassium fertilisers to reduce soil to plant C_r values.

Although the elimination of outlying values contributed to the lower degree of variability in the C_r values, uncertainty in assessment of mean values based on these data remains high for both buckwheat and soybean. Additionally, there was no correlation found between the observed variability and the number of samples used for C_r calculations. A possible explanation is that the farming management for buckwheat and soybean includes a crop rotation. Therefore, fields used for planting these crops may vary from year to year, using the fields with different remediation history.

It should also be considered that the transfer of ^{137}Cs to crops depends on weather conditions and the rate of fertilizers application. This can make it difficult to estimate the trend in the dynamics of a reduction in radionuclide uptake by plants. Depending on the weather conditions, the soil to plant C_r values observed in field conditions can differ from average values by a factor of 2–3 (Fesenko et al., 1997). Similarly, depending on the rate of potassium fertiliser applications, ^{137}Cs transfer to crops can vary from that observed under standard agricultural practice by a factor of 1.5–3. On the other hand, if fertilisers are applied in doses lower than that used for remediated lands, this could lead to the higher soil to plant C_r values. This effect is not so pronounced for paddy fields where technologies are standardised, and the effect of weather conditions is lower.

The data for all crops have been merged to derive a relationship between the ^{137}Cs C_r for the crops considered in this study (Table 7).

These ratios have been calculated separately for each year and each crop. There are some clear differences between the transfers of ^{137}Cs to the crops (Table 7). The highest ^{137}Cs transfer was to soybean, followed by buckwheat and finally to brown rice.

As mentioned in section 2.1, the data on radiocaesium concentrations in the crops for 2011 were very limited and included only data for brown rice sampled on selected representative fields along with measurements of air dose rates (Fukushima prefecture, 2011). No data are available for the other crops.

As information radiocaesium concentrations in the soils was not available, the concentrations of ^{137}Cs in brown rice were calculated for each field (indexed further with "*k*") based on air dose data (See Eqs. (1)–(5)). Thus, the dose-rate conversion coefficient for a reference depth distribution of radionuclide (plane radiation source) in the above equations (1)–(5) should be replaced with the similar dose-rate conversion coefficient (K^{k}_{soil}) of 2.93×10^{-4} and 1.06×10^{-4} μSv/h per Bq/

Table 6
Aggregated transfer factor values to the weed at the sampling sites in June–December 2011, (Bq kg^{-1})/(kBq m^{-2}), FW.

Site ID	GM	GSD	AM	SD	Min	Max	N[a]
2–1	2.22	2.2	3.2	0.81	0.57	21.0	60
2–2	1.82	2.6	2.9	0.97	0.38	13.4	55
2–3	5.3	2.0	6.6	0.67	1.6	19.4	17
2–4	4.83	2.0	6.0	0.71	1.3	17.4	25
2–6	3.83	1.8	5.0	0.93	0.9	18.5	33
2–7	0.8	2.3	1.9	0.65	0.2	6.8	58
2–8	1.48	1.9	2.7	0.65	0.45	9.6	56
2–9	1.31	2.6	2.1	0.93	0.3	8.4	44
4–3	2.92	2.6	4.5	0.97	0.39	19.4	47
All sites							
Fresh weight	2.3	1.2	3.5	1.7	0.2	21	
Dry weight	11.5	1.2	17.7	8.29	1	100	

[a] Number of data point used after outlining procedure.

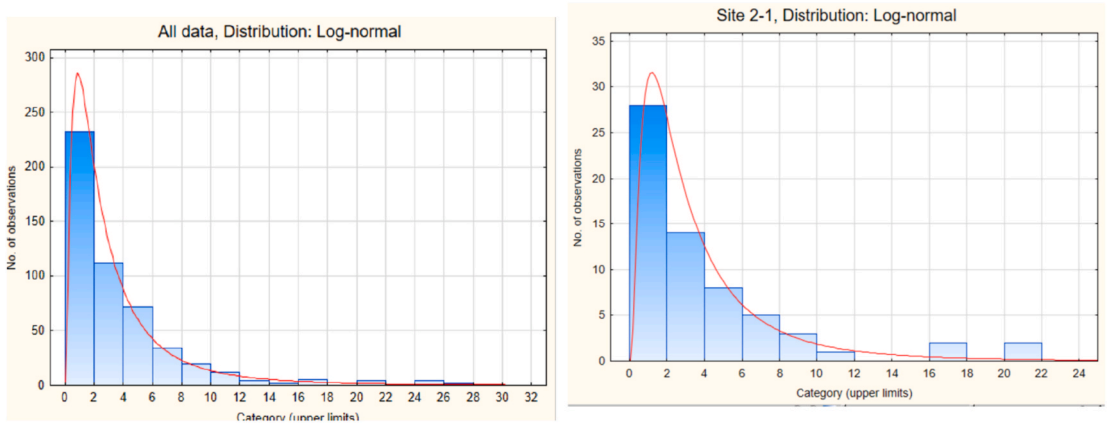

Fig. 7. Examples of the distributions of the ^{137}Cs aggregated transfer factors for the weed leaves in June–December 2011.

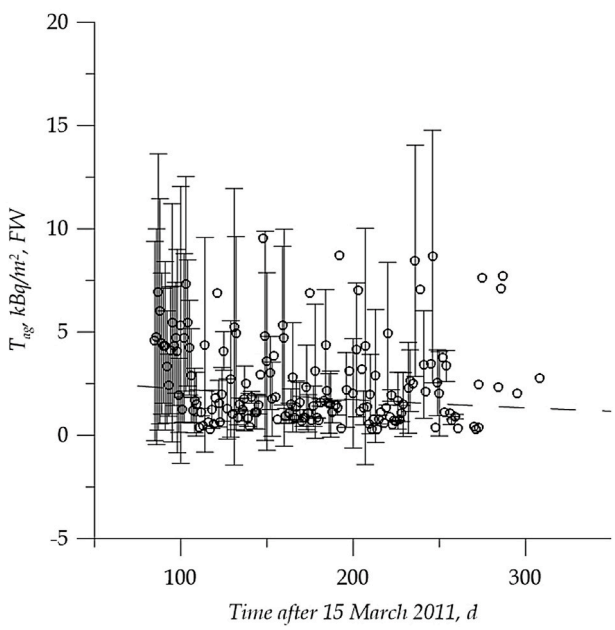

Fig. 8. T_{ag} values of ^{137}Cs transfer from soil to the weed leaves measured in June–December 2011. The bars represent standard deviations for each date point. Dashed line is the exponential fit.

kg for ^{134}Cs and ^{137}Cs, respectively, for a reference depth of radionuclide distribution in the soil of 15 cm (Bellamy et al., 2019).

$$C_r^k = \frac{Q_{rice}^k}{Q_{soil}^k} \tag{6}$$

where:

$$Q_{soil}^k = \frac{E_{air}^k}{\sum_i K_{soil}^k * \exp(-\lambda_i * t)} .$$

The geometric mean of soil to rice C_r value for 2011 estimated based on this approach was 1.83×10^{-2} with the geometric standard deviation around that mean of 1.57, whereas the arithmetic mean amounted (2.0 ± 1.0) × 10^{-2}. These values were around 3-fold higher than those observed for rice in 2012, reflecting a combined effect of ageing and remediation.

The data for 2012–2016 obtained in the study for brown rice, buckwheat and soybean demonstrate that the C_r values show a consistent downward trend (Fig. 10).

Both the two component and one component loss models were used to fit observed variations with the time in the C_r values for buckwheat, brown rice and soybean, and most significant approximations are shown in Fig. 10.

For 2012–2016, the first half-lives of ^{137}Cs soil to plant C_r values amounted to 1.0 year, and 2.4 years for buckwheat and soybean, respectively. For brown rice the half-life of 0.44 year estimated for 2011–2016 was shorter, likely because the data for 2011 were included in the analysis. The first half-lives of the two component loss models likely reflect the combined effect of both remediation and fixation of ^{137}Cs in the soil, whilst further reduction of ^{137}Cs C_r values was largely due to the decrease of radiocaesium bioavailability in the soil. Therefore, the second half-lives for buckwheat, rice and soybean were as long as 7.4, 1.7 and 6.3 years, respectively.

These data are consistent with other investigators' results, obtained both in Japan and in Europe. For example, Tagami and Uchida (2015) recently reported effective half-life values for ^{137}Cs concentrations in giant butterbur and field horsetail of 270–453 days that were measured in 2012–2014.

In the Chernobyl affected areas, Fesenko et al. (1995) have studied the reduction in ^{137}Cs concentrations in foodstuffs and fodder crops produced in the Bryansk and Kaluga regions of Russia that were contaminated after the Chernobyl accident. For the period of 1987–1989 (2–4 years after the depositions), the calculated effective half-lives for grains, hay and root crops were typically from one to three years, i.e. were similar to those reported in this paper. For the period 1990 to 1992 (4–6 years after the Chernobyl accident) the effective half-lives for the crops planted in the areas with intensive remediation varied between 1.0 and 7.3 years. It is known that the fixation of caesium by the mineral and organic fractions of soils plays an important role in reducing its availability for uptake by plants (Tamura, 1964; Cremers et al., 1988; Takeda et al., 2013; Tsukada, 2014; Tagami et al., 2018). The studies undertaken in areas of Russia most affected by the Chernobyl depositions also suggest that the reduction of the soil to plant ^{137}Cs C_r in areas where the effect of remediation could be excluded was within a period of one-and-a half to four years (Fesenko et al., 1996; Alexakhin et al., 2007). Similar values were derived from the presented data.

Pröhl et al. (2006) reviewed the data on reduction of ^{90}Sr and ^{137}Cs in different environments in Denmark, Germany and Austria. The data for global fallout was assessed starting from 1965. The data for 1986–1987, the first two years after the Chernobyl accident, were excluded from the analyses. They found that for plant and animal food products, the ecological half-lives were in the range of 4–6 and 10–20 years for caesium and strontium, respectively. At the same time these data do not allow direct comparison with our estimates as first years after the depositions were excluded.

The research performed in Austria by Mück (1994, 1997) suggests shorter ecological half-lives: 1.94 ± 0.32 year and 3.2 ± 0.7 for milk and

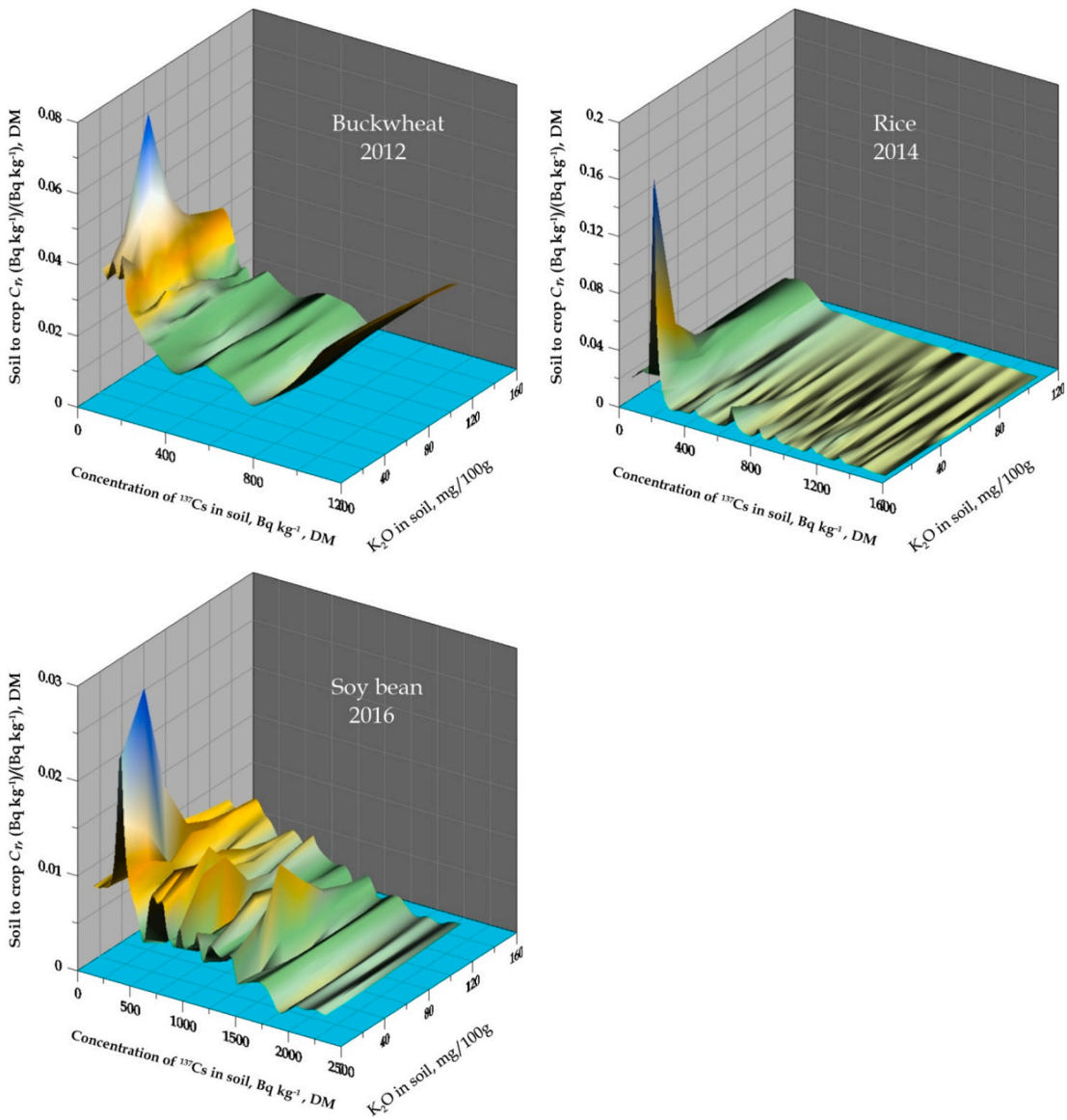

Fig. 9. Soil to crop ^{137}Cs C_r values in respect to the soil contamination and the concentration of exchangeable potassium in the soil.

Table 7
Ratios of C_r values for buckwheat, brown rice and soybean for 2012-2016, N = 6.

Parameters	Buckwheat/Rice	Buckwheat/Soybean	Soybean/Rice
GM	4.8	1.2	3.9
AM	4.9	1.3	4.4
St Deviation	1.5	0.4	2.7
Min	3.2	0.7	2.3
Max	6.2	1.7	9.1

cereals, respectively, comply with the estimates presented here. He also reported that ecological half-lives of radiocaesium concentrations in pasture vegetation ranged 1–4 years in the first 5–6 years after the deposition, followed by a slower decrease with an ecological half-life between 5 and 15 years. Smith et al. (1999, 2000) summarizing the above studies reported an increase of ecological half-lives of ^{137}Cs in terrestrial vegetation from 1 to 4 years during the first five years after the Chernobyl accident to 6–30 years in recent years. These data also comply with estimates of the half-lives given in this paper.

Of particular interest is whether or not the effective half-life observed for the period 2012 to 2016 is maintained in future years. Unfortunately, the data for the period 2011–2016 reported in this paper do not provide statistically robust data to answer this question, and this suggests that the period of observation may be too short for making the conclusions on the length of the second half-life.

4. Conclusions

The ecological half-lives of ^{131}I in the weed leaves in areas affected by the Fukushima accident ranged 3.8–4.2 d at the sampling sites where observations started not later than a week after the major deposition event, whereas for the sites where observations started three weeks after the depositions these values ranged 6.9–9.9 d. As for radiocaesium, these values were in a range from 7.2 to 8.7 d and from 29.4 to 42.2 d. These data are in reasonable agreement with the pre-Fukushima estimates. In the years following 2011, ^{137}Cs concentrations in crops decreased with an effective half-life typically in the order of one to two years, although there is still some uncertainty about the rate of decline in the effective half-life in crops from 2016. The available publications suggest that the rate of the reduction of soil to plant C_r is less than that observed during the initial years after the contamination, and this is consistent with the data reported in this paper. The data on reduction of

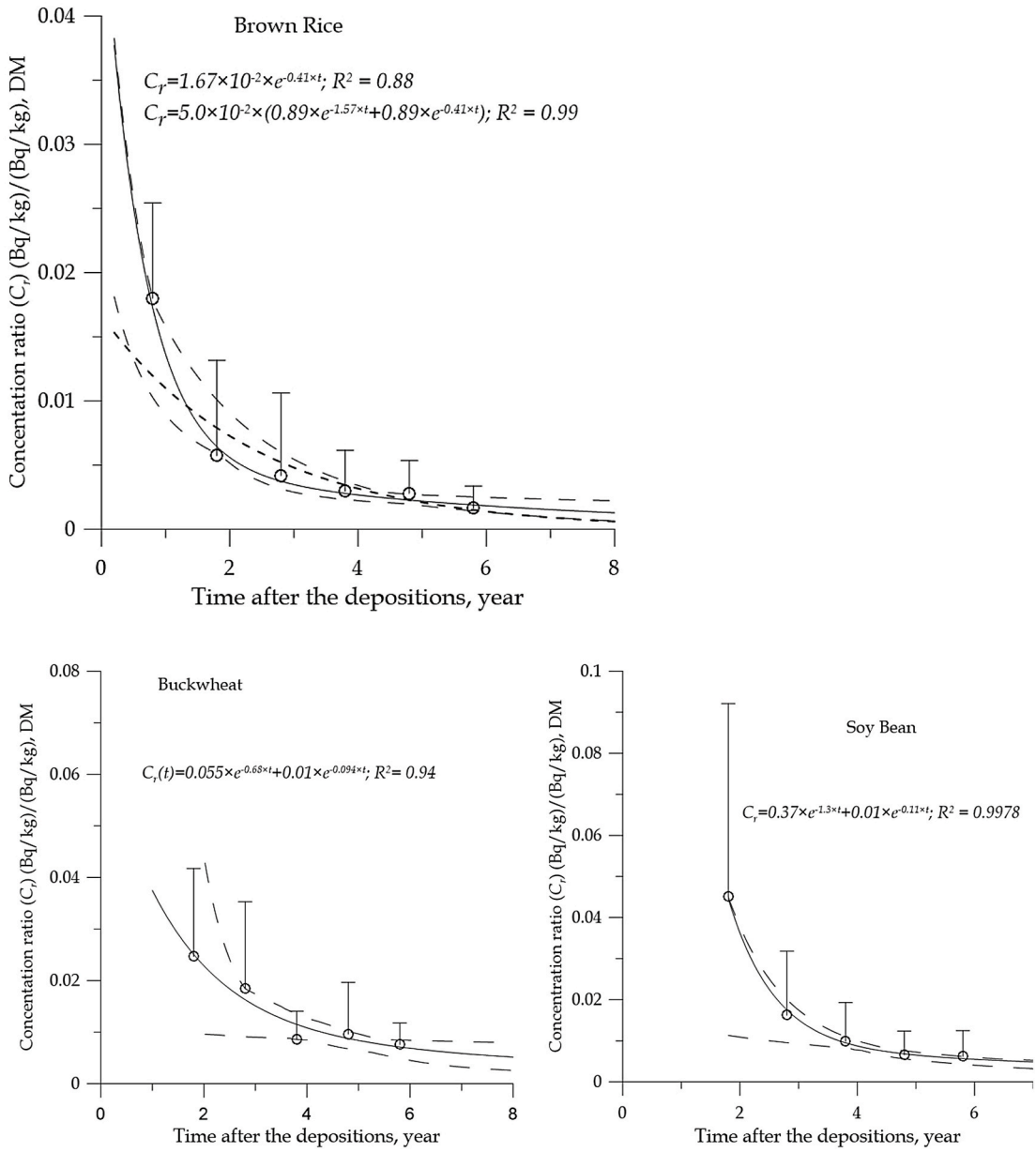

Fig. 10. Dynamics of soil to crop ^{137}Cs concentration ratios in the areas affected by the Fukushima accident. Dotted line for rice represent the exponential fit. Dashed lines provides the 95% confidence intervals of the fits.

the ambient equivalent dose rates obtained for the MEXT weed leaves sampling sites also complies with the pre-Fukushima data obtained mainly in Europe after the Chernobyl accident. The possible explanation is that the parameters of dose assessment models were dependent on similar factors, including fast penetration radionuclides in the top soil with wet depositions, weathering from plant surfaces and further growth of the biomass attenuating the radiation in the point of detection. The data presented also suggest that the ambient equivalent dose rate is a powerful tool that can be used for recovery of the data on deposition density of the main dose forming radionuclides, assessment of the C_r values if data on soil contamination are not available, and can be widely used to support decisions in case of a radiological or nuclear emergency. Besides immediately achieving a reduction in activity levels in plants, agricultural countermeasures and remedial options could also increase the rate at which these levels decline in subsequent years. This is an aspect of site restoration which should be seriously considered in both dose prediction models and in cost-benefit analysis of different intervention scenarios.

Declaration of competing interest

The authors declare that they have no known competing financial interests or personal relationships that could have appeared to influence the work reported in this paper.

Acknowledgment

This work was partly supported by the International Atomic Energy Agency within the framework of the Coordinated Research Project D15015 on Response to Nuclear Emergency affecting Food and Agriculture. Any views expressed are not necessarily those of the IAEA.

References

Abe, S., Fujitaka, K., Fujimoto, K., 1980. Natural radiation in Japan. In: Gesell, T.F., Lowder, W.M. (Eds.), Department of Energy. Technical Information Center, Oak Ridge, TN (USA), pp. 1034–1048, 1980; pp. 1034-1048; Conference on natural radiation environment III; Houston, TX, USA; 23 - 28 Apr 1978.

Alexakhin, R.M., Fesenko, S.V., Sanzharova, N.I., 1996. Serious radiation accidents and the radiological impact on agriculture. Radiat. Protect. Dosim. 64, 37–42.

Alexakhin, R.M., Sanzharova, N.I., Fesenko, S.V., Spiridonov, S.I., Panov, A.V., 2007. Chernobyl radionuclide distribution, migration, and environmental and agricultural impacts. Health Phys. 93 (5), 418–426.

Bellamy, M.B., Dewji, S.A., Leggett, M.R., Hiller, W., Veinot, K., Manger, R.P., Eckerman, K.F., Ryman, J.C., Easterly, C.E., Hertel, N.E., Stewart, D.J., 2019. Federal Guidance Report No. 15 External Exposure to Radionuclides in Air, Water and Soil. External Dose Rate Coefficients for General Application. U.S. Environmental Protection Agency, Washington. EPA 402-R-19-002.

Chaisan, K., Smith, J., Bossew, P., Kirchner, G., Laptev, G., 2013. Worldwide isotope ratios of the Fukushima release and early-phase external dose reconstruction. Sci. Rep. 3 (2520), 1–10.

Cremers, A., Elsen, A., De Preter, P., Maes, A., 1988. Quantitative analysis of radiocaesium retention in soils. Nature 335, 247–249.

Eckerman, K.F., Ryman, J.C., 1993. External Exposure to Radionuclides in Air, Water and Soil, Federal Guidance Report No. 12. US Environmental Protection Agency, Washington, DC.

Fesenko, S.V., Colgan, P.A., Sanzharova, N.I., Lissianki, K.B., Vazquez, C., Guardans, R., 1997. The dynamics of the transfer of caesium-137 to animal fodder is areas of Russia affected by the Chernobyl accident and resulting doses from the consumption of milk and milk products. Radiat. Protect. Dosim. 69 (4), 289–299.

Fesenko, S.V., Alexakhin, R.M., Spiridinov, S.I., Sanzharova, N.I., 1995. Dynamics of ^{137}Cs concentration in agricultural products in areas of Russia subjected to contamination after the accident at the Chernobyl nuclear power plant. Radiat. Protect. Dosim. 60 (2), 155–166.

Fesenko, S.V., Jacob, P., Alexakhin, R., Sanzharova, N.I., Panov, A., Fesenko, G., Cecille, L., 2001. Important factors governing exposure of the population and countermeasure application in rural settlements of the Russian Federation in the long term after the Chernobyl accident. J. Environ. Radioact. 56, 77–98.

Fesenko, S.V., Sanzharova, N.I., Spiridonov, S.I., Alexakhin, R.M., 1996. Dynamics of ^{137}Cs bioavailability in a soil-plant system in areas of the Chernobyl nuclear power plant accident zone with a different physico-chemical composition of radioactive fallout. J. Environ. Radioact. 34, 287–313.

Geras'kin, S.A., Fesenko, S.V., Chernyeva, L.G., Sanzharova, N.I., 1994. Statistical method of empirical distribution analysis of the coefficient of radionuclide accumulation in plants. Agric. Biol. 1, 130–137 (in Russian).

Golikov, V., Balonov, M., Erkin, V., Jacob, P., 1999. Model validation for external doses due to environmental contaminations by the Chernobyl accident. Health Phys. 77, 654–661.

Golikov, V.Y., Balonov, M.I., Jacob, P., 2002. External exposure of the population living in areas of Russia contaminated due to the Chernobyl accident. Radiat. Environ. Biophys. 41, 185–193.

Hirose, K., 2013. Temporal variation of monthly 137Cs deposition observed in Japan: effects of the Fukushima Daiichi nuclear power plant accident. Appl. Radiat. Isot. 81, 325–329.

IAEA, 2001. Generic Models for Use in Assessing the Impact of Discharges of Radioactive Substances to the Environment, IAEA Safety Reports Series No. 19. International Atomic Energy Agency, Vienna.

IAEA, 2006. International Atomic Energy Agency. Environmental Consequences of the Chernobyl Accident and Their Remediation: Twenty Years of Experience. Report of the UN Chernobyl Forum Expert Group "Environment" (EGE). International Atomic Energy Agency, Vienna.

IAEA, 2009. Quantification of Radionuclide Transfer in Terrestrial and Freshwater Environments for Radiological Assessments, 1616. International Atomic Energy Agency, Vienna.

IAEA, 2010. Handbook of Parameter Values for the Prediction of Radionuclide Transfer in Terrestrial and Freshwater Environments, Technical Reports Series No. 472 Vienna. International Atomic Energy Agency, 2010.

IAEA, 2015. The Fukushima Daiichi Accident, Technical Volume 4/5 Radiological Consequences. International Atomic Energy Agency, Vienna.

Kato, H., Onda, Y., Gao, X., Sanada, Y., Saito, K., 2019. Reconstruction of a Fukushima accident-derived radiocesium fallout map for environmental transfer studies. J. Environ. Radioact. (in press).

Kato, H., Onda, Y., Gomi, T., 2012. Interception of the Fukushima reactor accident-derived ^{137}Cs, ^{134}Cs and ^{131}I by coniferous forest canopies. Geophys. Res. Lett. 39, L20403, 2012.

Kato, H., Onda, Y., Loffredo, N., Hisadome, K., Kawamori, A., 2017. Temporal changes in radiocesium deposition in various forest stands following the Fukushima Dai-ichi Nuclear Power Plant accident. J. Environ. Radioact. 116 (3), 449–457.

Khomutinin, Yu., Fesenko, S, Levchuk, S., Holiaka, D., Kashparov, V., 2020a. Optimising sampling strategies for emergency response: sampling of vegetation. J. Environ. Radioact. In this issue.

Khomutinin, Yu., Fesenko, S., Levchuk, S., Zhebrovska, K., Kashparov, V., 2020b. Optimising sampling strategies for emergency response: Soil sampling. J. Environ. Radioact. In this issue.

MAFF, 2013. Points to reduce radiocaesium concentration in rice at rice production fields, 2013 (in Japanese). http://www.maff.go.jp/j/kanbo/joho/saigai/pdf/130710_komeq17_rev.pdf.

MEXT, 2011. Ministry of Education, Culture, Sports, Science and Technology. Results of Airborne Monitoring Survey by MEXT in Iwate, Shizuoka, Nagano, Yamanashi, Gifu, and Toyama Prefectures, and Revision of the Past Airborne Monitoring Results by Refracting the Influences of Natural Radionuclides (2011).

MEXT, 2012a. Ministry of Education, Culture, Sports, Science and Technology. Compiled in Nuclear Regulation Authority website: https://radioactivity.nsr.go.jp/en/contents/6000/5706/24/ReadingsofenvironmentalmonitoringsampleJune1,2011-%20December31,201120121101.pdf.

MEXT, 2012b. Ministry of Education, Culture, Sports, Science and Technology 2012b. Compiled in Nuclear Regulation Authority website. http://radioactivity.nsr.go.jp/ja/contents/70006416/24/ReadingsofenvironmentalmonitoringsampleJune1,2011-%20December31,201120121101.pdf.

Mück, K., 1997. Long-term effective decrease of cesium concentration in foodstuffs after nuclear fallout. Health Phys. 72 (5), 659–673.

Mück, K., et al., 1994. Effective half-lives of I-and Cs-isotopes in grassland shortly after fallout. J. Environ. Radioact. 24 (2), 127–143.

Nagai, H., Chino, M., Terada, H., Katata, G., 2012. Atmospheric dispersion simulations of radioactive materials discharged from the Fukushima Daiichi nuclear power plant due to accident: consideration of deposition process. In: Kurihara, O., Akahane, K., Fukuda, S., Miyahara, N., Yonai, S. (Eds.), Reconstruction of Early Internal Dose in the TEPCO Fukushima Daiichi Nuclear Power Station Accident (Proc. 1st NIRS Symp. 2012. National Institute of Radiological Sciences, Chiba, pp. 137–138, 2012.

NRA, 2011. Nuclear regulation authority. Monitoring information of environmental radioactivity level. Readings at reading points out of 20 km zone of TEPCO Fukushima dai-ichi NPP. http://radioactivity.nsr.go.jp/en/list/195/list-1.html.

Onda, Y., Kato, H., Hoshi, M., Takahashi, Y., Nguyen, M., 2015. Soil sampling and analytical strategies for mapping fallout in nuclear emergencies based on the Fukushima Dai-ichi Nuclear Power Plant accident. J. Environ. Radioact. 139, 300–307.

Onda, Y., Swank, L., Shinano, T., Dercon, G., Lee Zhi Yi, A., Kato, H., Ohse, K., 2020. Soil and vegetation sampling approaches for agricultural systems during early stage of nuclear emergencies. J. Environ. Radioact. (in this issue).

Pröhl, G., Ehlken, S., Fiedler, I., Kirchner, G., Klemt, E., Zibold, G., 2006. Ecological half-lives of ^{90}Sr and ^{137}Cs in terrestrial and aquatic ecosystems. J. Environ. Radioact. 91 (1–2), 41–72.

Renaud, P.H., et al., 2012. Contamination of Japanese foodstuffs of terrestrial origin after the Fukushima nuclear accident and related dose assessments Part 1: foodstuff contamination. Radioprotection 48, 493–509.

Sanzharova, N.I., Fesenko, N.V., Alexakhin, R.M., Anisimov, V.S., Kuznetsov, V.K., Chernyayeva, L.G., 1994. Changes in the form of ^{137}Cs and its availability for plants as dependent on properties of fallout after the Chernobyl nuclear power plant accident. Sci. Total Environ. 154, 9–22.

Sheppard, S.C., Evenden, W.G., 1988. The assumption of linearity in soil and plant concentration ratios: an experimental evaluation. J. Environ. Radioact. 7, 221–247.

Sheppard, S., Evenden, W.G., 1990. Characteristics of plant concentration ratios assessed in a 64-site survey of 23 elements. J. Environ. Radioact. 11, 15–36.

Shinano, T., Hachinohe, M., Fesenko, S., 2020. Relationships between Ambient Dose Rate and Radionuclide Concentrations in Agricultural Plants Observed in Areas Affected by the Fukushima Daiichi Accident (This issue).

Simon, S.L., Ibrahim, S.A., 1987. The plant/soil concentration ratio for calcium, radium, lead and polonium: evidence for non-linearity with reference to substrate concentration. J. Environ. Radioact. 5, 123–142.

Smith, J.T., Comans, R., Beresford, N.J., Wright, S.M., Howard, B.J., Camplin, W.C., 2000. Chernobyl's legacy in food and water. Nature 405 (6783), 141-141.

Smith, J.T., Fesenko, S., Howard, B.J., Horrill, D., Sanzharova, N.I., Alexakhin, R.M., Elder, D.G., Naylor, Ch, 1999. Temporal change in fallout ^{137}Cs in terrestrial and aquatic systems: a whole ecosystem approach. ES T (Environ. Sci. Technol.) 33 (1), 49–54.

Tagami, K., Tsukada, H., Uchida, S., Howard, B.J., 2018. Changes in the soil to brown rice concentration ratio of radiocaesium before and after the Fukushima Daiichi nuclear power plant accident in 2011. ES T (Environ. Sci. Technol.) 52, 8339.

Tagami, K., Uchida, S., 2015. Effective half-lives of ^{137}Cs in giant butterbur and field horsetail, and the distribution differences of potassium and ^{137}Cs in aboveground tissue parts. J. Environ. Radioact. 141, 138–145.

Takahashi, S. (Ed.), 2014. Radiation Monitoring and Dose Estimation of the Fukushima Nuclear Accident. Springer, Japan.

Takeda, A., Tsukda, H., Nakao, A., Takaku, Y., Hisamitsu, S., 2013. Time-dependent changes of phytoavailability of Cs added to allophanic Andosols in laboratory cultivations and extraction tests. J. Environ. Radioact. 122, 29–36.

Tamura, T., 1964. Selective sorption reaction of caesium with soil minerals. Nucl. Saf. 5, 262–268.

Tsukada, H., 2014. Behavior of radioactive cesium in soil with aging. Jpn. J. Soil Sci. Plant Nutr. 85, 77–79 (In Japanese).

Uchida, S., Tagami, K., 2007. Soil-to-plant transfer factors of fallout ^{137}Cs and native ^{133}Cs in various crops collected in Japan. J. Radioanal. Nucl. Chem. 273, 205–210.

UNSCEAR, 2013. United Nations Scientific Committee on the Effects of Atomic Radiation, Report to the General Assembly. Scientific Annex A. United Nations, New York, 2014.

Yamamura, K., Fujimura, S., Saito, T., Ishikawa, T., Arai, M., Ota, T., Shinano, T., 2018. A statistical model for estimating the radiocaesium transfer factor from soil to brown rice using the soil exchangeable potassium content. J. Environ. Radioact. 195, 114–125.

Yoshimura, K., Saegusa, J., Sanada, Yu, 2020. Initial decrease in the ambient dose equivalent rate after the Fukushima accident and its difference from Chernobyl. Sci. Rep. 10, 3859–3868.